

Valence-Band-Offset Controversy in HgTe/CdTe Superlattices: A Possible Resolution

N. F. Johnson, P. M. Hui, and H. Ehrenreich^(a)

Division of Applied Sciences, Harvard University, Cambridge, Massachusetts 02138

(Received 12 July 1988)

The valence-band-offset controversy in HgTe/CdTe superlattices can be simply resolved. It is shown that, while the superlattice becomes semimetallic with increasing valence-band offset, it reverts to semiconducting behavior as the offset is increased yet further. The observed electron-cyclotron mass and the band gap can be better explained for the offset of 350 meV measured by photoemission than for the smaller offset ~ 40 meV which coincidentally is also in fair agreement with the magneto-optical data.

PACS numbers: 73.40.Lq, 73.20.At, 73.20.Dx

The dilemma posed by the differing valence-band offsets Λ in HgTe/CdTe superlattices (SL) obtained from room-temperature photoemission ($\Lambda \approx 350$ meV)¹ and low-temperature magneto-optical experiments ($\Lambda \approx 40$ meV)² can be resolved in favor of the larger Λ by showing, as we do here, that the effective mass and the band gap obtained by Berroir *et al.*² are consistent with the value $\Lambda \approx 350$ meV. As noted previously³ the conduction and valence bands of the semiconducting superlattices cross as Λ is increased from small values and render the material semimetallic. What has been missed is the fact that the superlattice again becomes semiconducting as Λ is increased further for the layer widths corresponding to the SL described in Ref. 2.

These results are obtained with use of the envelope-function approach which has recently been criticized^{4,5} because of its reliance on $\mathbf{k} \cdot \mathbf{p}$ perturbation theory. Indeed, the bulk $k=0$ basis set used here is limited to that of the Kane model. The results have been questioned on the grounds that a broader width of the bulk Brillouin zone than that adequately described by the model would play a role in the SL electronic structure. However, as we have recently shown,⁶ the results obtained using the extended basis comprising ~ 50 bulk wave functions at $k=0$, which would be expected to describe the requisite region of the Brillouin zone adequately, are essentially the same as those for the limited

basis set exemplified by the Kane model, even for narrow layer width. This approach has been shown to yield quantitative results for effective masses and optical-absorption coefficients for a variety of 3–5 and 2–6 SL's.^{7,8} The theoretical approach outlined in Ref. 7 can therefore be regarded as applicable to the present considerations. The calculations, however, neglected strain effects.

Figure 1 shows the relative alignment of the bulk HgTe and CdTe band edges (Γ_6 and Γ_8) schematically. The band offset Λ is defined to be positive. The potential well formed by the Γ_6 edge (solid line) becomes shallower with increasing Λ , whereas that for the Γ_8 edge (dashed line) becomes deeper.

The present calculations refer to the 100-Å HgTe/36-Å CdTe SL considered in the magneto-optical experiments of Ref. 2. The only input consists of the constituent bulk parameters listed in Table I. These parameters determine the bulk momentum matrix elements for each material within the Kane model. They differ by less than 10% and will therefore be taken to have the same average value for both materials.

Figure 2 shows the energies of the C1, LH1, HH1, HH2, and HH3 (C denotes conduction, LH light hole, and HH heavy hole) bands at $\mathbf{K}=0$ (\mathbf{K} is the SL wave vector) as a function of band offset Λ . The zero of energy is taken to be the valence-band maximum for $\Lambda=0$. At zero offset the electrons are located in a quantum well of finite depth, whereas the holes see no potential varia-

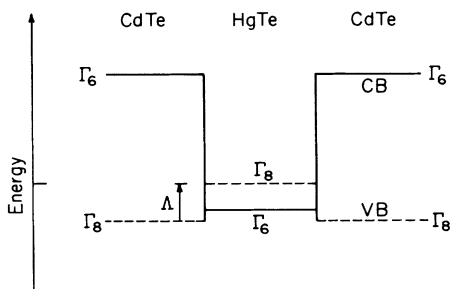


FIG. 1. The relative alignment of the bulk HgTe and CdTe band edges. The valence-band offset Λ is defined as the difference between the HgTe and CdTe Γ_8 valence-band maxima.

TABLE I. Parameters for bulk CdTe and HgTe used in the present calculations.

	CdTe	HgTe
Electron mass (m_0)	0.11	0.031 ^a
$E(\Gamma_6) - E(\Gamma_8)$ (eV)	1.6	-0.3
Spin-orbit splitting (eV)	0.9	1.0
Heavy-hole mass (m_0) ^b	0.7	0.7

^aReference 9.

^bReference 10. We use the heavy-hole masses along the [111] direction.

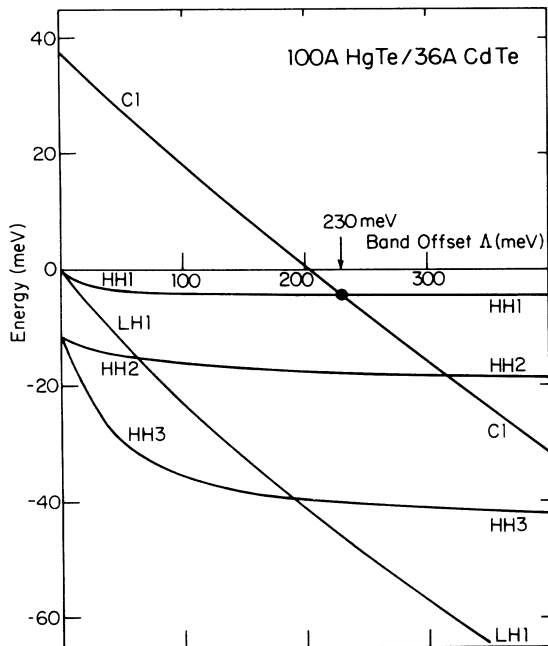


FIG. 2. The energies of the bands C1, LH1, HH1, HH2, and HH3 at $\mathbf{K}=0$ as a function of band offset Λ for 100-Å HgTe/36-Å CdTe superlattice (see Ref. 2).

tion. With increasing Λ the electron energies become less positive, whereas the hole energies become more negative as the well becomes more substantial. The most dramatic feature is the rapid variation of the C1 and LH1 bands relative to the HH bands. This behavior is associated with the light bulk effective masses characterizing the former bands. The heavy-hole bulk mass is sufficiently large that the potential well seen by the HH particles is effectively infinite for $\Lambda \geq 100$ meV and the values become virtually constant. The C1 and HH1 bands cross at 230 meV, the HH1 electrons are transferred to the C1 band, and the SL becomes semimetallic.

The behavior of the minimum band gap E_g is determined by the SL band structure along K_{\perp} perpendicular to the layers. Figure 3 shows E_g as a function of Λ and directly above the appropriate energies a sketch of the SL band structure for the offset indicated by the arrows. The figure divides itself into three regimes. For $0 < \Lambda < 230$ meV the SL is a semiconductor (SC) with a direct gap at $\mathbf{K}=0$ and with C1 and HH1 the lowest conduction band and highest valence band, respectively. For $230 < \Lambda < 295$ meV the superlattice is semimetallic.¹¹

The new and remarkable feature we note here is the third region in which the SL becomes semiconducting once again for $\Lambda > 295$ meV as a result of the continued downward shift of the C1 band and a resulting uncrossing of the C1 and HH1 bands. The band gap in this region is still direct but, as shown in Fig. 3, it occurs at the

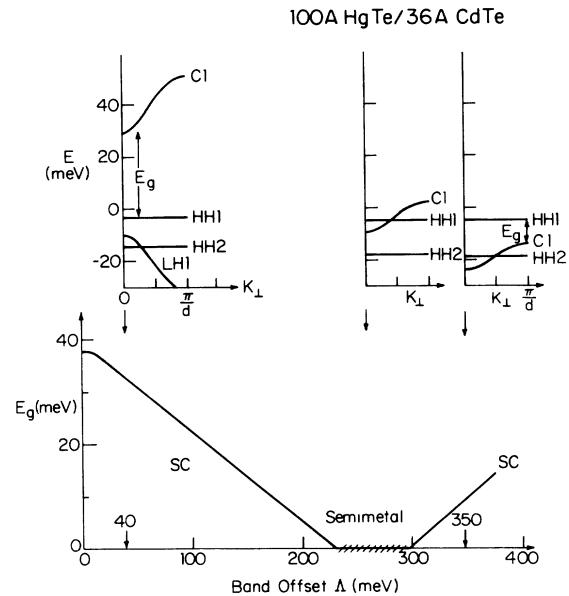


FIG. 3. The band gap, E_g , as a function of the band offset Λ for 100-Å HgTe/36-Å CdTe superlattice. Also shown are the band structures in the \perp direction at $K_{\parallel}=0$ for $\Lambda=40$, 260, and 350 meV.

SL Brillouin-zone face $K_{\perp}=\pi/d$, where d is the SL period. (C1 and HH1 just touch at $\Lambda=295$ meV.) In this region C1 becomes a valence and HH1 a conduction miniband. In the absence of conduction-band electrons, $E_g=10$ meV for $\Lambda=350$ meV.

The behavior of the in-plane electron effective mass m_{\parallel} and the corresponding band structure along K_{\parallel} as a function of band offset is shown in Fig. 4 using the same format as that of Fig. 3. The behavior of the band structure is quite reminiscent of that encountered in $\text{Hg}_x\text{Cd}_{1-x}\text{Te}$ alloys as a function of Hg concentration x . With increasing band offset the band gap decreases until the C1 and HH1 bands just touch at 230 meV and the E vs K dispersion becomes linear. Subsequently they exchange roles in that HH1 becomes the conduction band and C1 the valence band. This behavior results from the $\mathbf{k} \cdot \mathbf{p}$ interaction between the two bands along the \parallel direction. They do not interact along the \perp direction. For $\Lambda < 230$ meV, m_{\parallel} is roughly proportional to E_g , and formally vanishes at the intersection. The effective mass m_{\parallel} shown in the subsequent region is that of the new conduction band HH1 at $\mathbf{K}=0$.

The experimental electron-cyclotron mass ($m_c^*/m_0 = 0.017 \pm 0.003$) at 1 T,² extrapolated to vanishing magnetic field (0.015 ± 0.003) is also shown with its error bars at both $\Lambda=40$ and 350 meV. The magnitude is somewhat larger than the band-edge, $\mathbf{K}=0$, value at $\Lambda=350$ meV. The energy gap is seen from Fig. 3 to have a value 10 meV as compared to the quoted² “ ~ 20 meV.” Since unintentionally doped n -type samples have

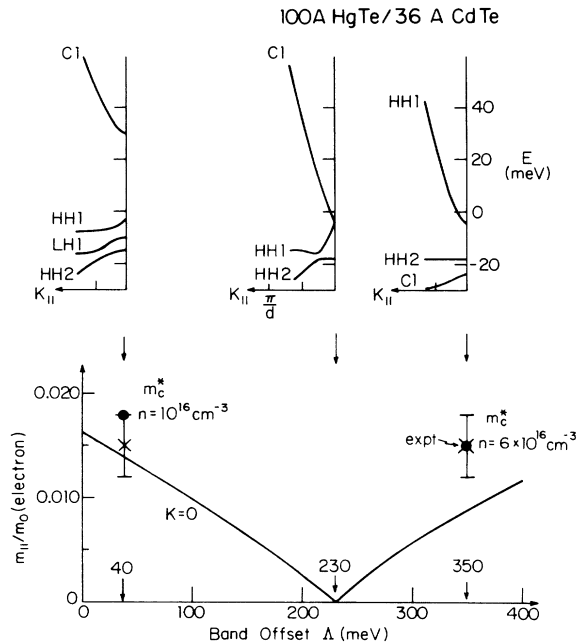


FIG. 4. Bottom: The in-plane effective mass m_{\parallel} at $\mathbf{K}=0$ (solid line) as a function of the band offset Λ for 100-Å HgTe/36-Å CdTe superlattice. The experimental value (crosses) of the cyclotron mass m_c^* in the limit of zero field is shown with its error bars and the theoretical values (solid circles) of m_c^* with use of $6 \times 10^{16} \text{ cm}^{-3}$ for $\Lambda=350 \text{ meV}$ and 10^{16} cm^{-3} for $\Lambda=40 \text{ meV}$. Top: The band structures in the \parallel direction at $K_{\perp}=0$ for $\Lambda=40, 230,$ and 350 meV .

carrier densities $n \gtrsim 10^{16} \text{ cm}^{-3}$, an electron density was calculated that would produce a value of m_c^*/m_0 consistent with the experimental mass (Ref. 2 does not cite a precise value of n). As shown in Fig. 4 the requisite electron concentration for $\Lambda=350 \text{ meV}$ is $6 \times 10^{16} \text{ cm}^{-3}$. (The extremal values of m_c^*/m_0 at $K_{\perp}=0$ and π/d are almost identical because the HH1 constant energy surfaces are calculated to be nearly cylindrical. This point will be fully discussed elsewhere.) The corresponding Fermi energy lies 17 meV above the band minimum. Thus no interband transitions should be observed below 27 meV, in accord with experiment.² The same calculation for $\Lambda=40 \text{ meV}$ and $n=10^{16} \text{ cm}^{-3}$ yields $m_c^*/m_0=0.018$, quite close to the $\Lambda=350 \text{ meV}$ value. This observation provides some insight into the cause of the band-offset controversy: Both values of Λ coincidentally lead to similar results. The value of E_g , however, is 33 meV for $\Lambda=40 \text{ meV}$ and therefore larger than the approximate experimental value cited in Ref. 2.

Note that for $\Lambda=350 \text{ meV}$, a smaller unintentional doping corresponding to $n=2 \times 10^{16} \text{ cm}^{-3}$ yields $m_c^*/m_0=0.012$. This result still falls within the experimental error² cited for m_c^* , and shows the precise value of n to be relatively unimportant.

Because of the unexpected semimetal to semiconductor transition at $\Lambda=295 \text{ meV}$, the data of Ref. 2 are seen to be *better* explained by an offset $\Lambda \approx 350 \text{ meV}$ (or possibly even a slightly larger value) than the smaller $\Lambda=40 \text{ meV}$. The semiconductor and semimetal transitions described here depend sensitively on the quantum well width for a given narrow barrier and band offset. For $\Lambda=350 \text{ meV}$ and the well width of the SL in Ref. 2 reduced to 50 \AA , C1 would be above HH1 and E_g would lie at $\mathbf{K}=0$, as is commonly assumed. The dependence of E_g on composition, strain, and temperature¹² requires further investigation.

We are grateful to K. C. Hass and J. R. Meyer for helpful discussions. We also thank R. J. Wagner for correcting our interpretation of the magneto-optical data. This research was supported by the U.S. Defense Advanced Research Projects Agency under Contract No. ONR N00014-86-K-0033 and the Joint Services Electronics Project under Contract No. ONR N00014-84-K-0465.

(a)To whom all correspondence should be addressed.

¹S. P. Kowalczyk, J. T. Cheung, E. A. Kraut, and R. W. Grant, Phys. Rev. Lett. **56**, 1605 (1986); T. M. Duc, C. Hsu, and J. P. Faurie, Phys. Rev. Lett. **58**, 1127 (1987); C. K. Shih and W. E. Spicer, Phys. Rev. Lett. **58**, 2594 (1987).

²J. M. Berroir, Y. Guldner, J. P. Vieren, M. Voos, and J. P. Faurie, Phys. Rev. B **34**, 891 (1986); see also J. M. Berroir, Y. Guldner, and M. Voos, IEEE J. Quantum Electron. **22**, 1793 (1986).

³C. A. Hoffman, J. R. Meyer, F. J. Bartoli, J. W. Han, J. W. Cook, Jr., J. F. Schetzina, and J. N. Schulman, to be published. We are grateful to J. R. Meyer for communicating these results prior to publication.

⁴M. Jaros, Phys. Rev. Lett. **60**, 2560 (1988).

⁵G. Bastard, Phys. Rev. Lett. **60**, 2561 (1988).

⁶N. F. Johnson, H. Ehrenreich, G. Y. Wu, and T. C. McGill, Phys. Rev. B (to be published).

⁷N. F. Johnson, H. Ehrenreich, K. C. Hass, and T. C. McGill, Phys. Rev. Lett. **59**, 2352 (1987).

⁸N. F. Johnson, H. Ehrenreich, and R. V. Jones, Appl. Phys. Lett. **53**, 180 (1988).

⁹Y. Guldner, C. Rigaux, M. Grynberg, and A. Mycielski, Phys. Rev. B **8**, 3875 (1973).

¹⁰J. N. Schulman and Y. C. Chang, Phys. Rev. B **33**, 2594 (1986).

¹¹This discussion assumes that the band crossings and uncrossings responsible for the semiconductor and semimetal transitions are confined to the region around $\mathbf{K}=0$ considered here and that other regions of the Brillouin zone have larger gaps. This is inferred from the bulk band structures, their relative energetic positions, and the fact that the SL bands are described qualitatively by folding bulk bands into the new Brillouin zone.

¹²D. H. Chow, J. O. McCaldin, A. R. Bonnefoi, T. C. McGill, I. K. Sou, and J. P. Faurie, Appl. Phys. Lett. **51**, 2230 (1987).